journal

J. Am. Ceram. Soc., 73 [6] 1555-65 (1990)

Superplastic Flow of Two-Phase Ceramics Containing Rigid Inclusions—Zirconia/Mullite Composites

Chong K. Yoon* and I-Wei Chen*

Department of Materials Science and Engineering, University of Michigan, Ann Arbor, Michigan 48109-2136

A continuum theory for non-Newtonian flow of a two-phase composite containing rigid inclusions is presented. It predicts flow suppression by a factor of $(1 - V)^q$, where V is the volume fraction of the rigid inclusion and q depends on the stress exponent and the inclusion shape. Stress concentrations in the rigid inclusion have also been evaluated. As the stress exponent increases, flow suppression is more pronounced even though stress concentration is less severe. To test this theory, superplastic flow of zirconia/mullite composites, in which zirconia is a soft, non-Newtonian superplastic matrix and mullite is a rigid phase of various size, shape, and amount, is studied. The continuum theory is found to describe the two-phase superplastic flow reasonably well. [Key words: flow, composites, mullite, zirconia.]

I. Introduction

SUPERPLASTICITY of fine-grain polycrystals has been widely reported for metals[1] and, most recently, for ceramics.[2-4] Although a majority of superplastic materials contain two phases, definitive studies of constitutive relations of multiphase alloys and ceramics at elevated temperatures are few. From a theoretical viewpoint, Chen has drawn attention to two prototype behaviors in two-phase superplastic flow.[5] The first type is the classical composite behavior in which each constituent phase deforms according to its own constitutive relation. In such case, the deformation resistance of the composite is bounded by the deformation resistances of the two constituent phases. Corresponding behavior of this kind in linear elasticity, viscoelasticity, and Newtonian fluid flow is well understood. In the second type, stress-driven kinetic demixing, due to different mobilities of common constituent atoms or ions shared by two phases, is predominant. As a consequence, migration of phase boundaries occurs which, in turn, alleviates back stresses and solute segregation. Diffusional flow is thus facilitated, lowering the deformation resistance in some microduplex composites to a value below those of both constituent phases.[6] To emphasize the distinct physical nature governing two-phase superplastic flow, Chen has suggested that the first type be named rheological flow, and the second, interdiffusional flow. Evidence of both types of behavior, mostly in metals, was cited by Chen from the literature.[5]

Rheological superplastic flow may be modeled using continuum mechanics. For creep and superplastic flow, a correct treatment must take into account the non-Newtonian nature of the constitutive laws. Such nonlinear problems are generally very difficult and rarely amenable to an analytical treatment, except in special cases.[5] One such case, of particular interest for structural applications, is a soft power-law creeping matrix reinforced by rigid inclusions. It can be shown that the composite follows a similar power-law relation between stress and strain rate, with the same stress exponent, but with a different prefactor whose value depends on the shape and the volume fraction of inclusions. A theory addressing this problem is presented here and the superplastic flow of a family of (soft) zirconia/(rigid) mullite composites is used to elucidate such behavior.

Several considerations on the merit of the zirconia/mullite system as a model composite for the present purpose should be mentioned to provide a background of our study. First, zirconia has been reported to deform superplastically at high temperatures.[2,3] While the composition typically used for such studies has been 3Y-TZP (97 mol% ZrO_2–3 mol% Y_2O_3), which contains 90 vol% tetragonal phase and 10 vol% cubic phase, we have chosen a lower yttria composition of 2 mol% (2Y-TZP) so that only the tetragonal phase is present. It was expected, and indeed verified in our study, that 2Y-TZP is superplastic with a very low deformation resistance. On the other hand, mullite ($3Al_2O_3 \cdot 2SiO_2$) is known for very good creep resistance. For example, single crystals of mullite stressed along the c-axis do not deform plastically at 1500°C to 900 MPa, and the diffusional creep rate of polycrystalline mullite (grain size $\approx$ 3 to 4 μm) is $\sim 6 \times 10^{-8}$/s at 1400°C at 90 MPa.[7] Thus, these two phases have drastically different deformation resistances, with mullite being the rigid one. Nevertheless, the two oxides have very similar elastic constants: Young's modulus around 210 GPA and shear modulus around 80 GPa, for both. Since thermal stresses can be ignored at elevated temperatures, this means that in superplastic flow the stress distribution in the zirconia/mullite composite will be entirely governed by plasticity, which is the assumption taken by our theory. Chemically, we have also found 2Y-TZP and mullite to be compatible with little mutual solubility. This implies that the phase compositions and phase fractions of the two are independent of temperature in a composite of a given composition, which simplifies the mechanical analysis. Lastly, an additional advantage of mullite as a strengthening phase is its morphological variability. It is known from our preliminary work that the grain shape of mullite varies considerably from an equiaxed shape at the alumina-rich compositions to an elongated shape at the silica-rich compositions. It thus allows us to study the shape effect in strengthening. Taken in toto, it becomes obvious that zirconia/mullite composites afford an excellent model system in which the effects of a rigid second phase of various fractions and shapes can be systematically explored.

R. Raj—contributing editor

Manuscript No. 198337. Received June 7, 1989; approved December 1, 1989.

Presented at the 90th Annual Meeting of the American Ceramic Society, Cincinnati, OH, May 5, 1988 (Basic Science Division, Paper Nos. 235-B-88 and 236-B-88).

Supported by the U.S. Department of Energy under Grant No. DE-FG02-87ER45302.

*Member, American Ceramic Society.

II. Theory of Composites Containing Rigid Inclusions

(1) Statement of Problem

We distinguish the matrix phase from the included phase and let the included phase be rigid. The matrix phase is incompressible and obeys a power law

$$\dot{\varepsilon} = \alpha(\sigma/\sigma_0)^n \tag{1}$$

in uniaxial tension. Here $\dot{\varepsilon}$ is the tensile strain rate, σ is the tensile stress, α is a reference strain rate, σ_0 is a reference stress, and n is no less than unity. This form can be generalized to multiaxial deformation, governed by an effective stress, in the standard way described in theory of plasticity.[8] By necessity, the composite is incompressible itself and obeys a similar power law in uniaxial tension

$$\dot{E} = A\alpha(\Sigma/\sigma_0)^n \tag{2}$$

where $\dot{E}$ is the composite strain rate, Σ is the macroscopic stress, and A is a dimensionless constant less than unity. Our task is to find A as a function of V, the volume fraction of inclusions.

The flow behavior of a Newtonian fluid ($n = 1$), with dilute rigid spherical inclusions, is well-known, i.e., $A = 1 - 2.5V$.[9,10] The solution of A at higher inclusion concentrations requires the use of an incremental scheme of computation.[11-14] It is recognized in this scheme that the addition of more rigid inclusions to a concentrated mixture results in a lesser degree of hardening since the mixture already has a fairly high flow stress which lessens the extent of stress concentration in the rigid inclusions. If the solution of the deformation fields in an inclusion is already known, then a mean field approximation in which the mixture is treated as an effective continuum for the inclusion can be adopted. For self-consistency, the macroscopic properties of the composite itself are assigned to the effective medium. This method is repeated while more inclusions are added to the mixture. In a linear material the inclusion problem is well-known, from which the theory predicts $A = (1 - V)^q$, where $q = 2.5$ for spherical rigid inclusions.[11-14] Note that the above power-law form reduces to the linear form when V approaches zero. The extension of this type of approach to nonlinear problems should lead to a similar prediction, but the value of q needs to be determined as a function of stress exponent of the matrix and the shape of the inclusion. This task is made easier by recognizing a connection between q in the self-consistent equation and the stress concentration factor in the inclusion.

(2) The Self-Consistent Equation

Let us consider that each inclusion, on average, has a stress concentration factor k over that of the applied tensile stress Σ. Then the average stress remaining in the matrix is $(1 - kV)/(1 - V)$ times the applied stress. Inasmuch as inclusions are rigid and do not contribute to the macroscopic deformation, the strain rate of the composite due to matrix alone may be expressed as

$$\dot{E} = (1 - V)\alpha[(1 - kV)/(1 - V)(\Sigma/\sigma_0)]^n \tag{3}$$

The above form is due to Chen and Argon.[15]

In the limit of small V, the above form can be expanded to the first order in V

$$\dot{E} = (1 - qV)\alpha(\Sigma/\sigma_0)^n \qquad (V \sim 0) \tag{4}$$

where

$$q = 1 + (k - 1)n \tag{5}$$

In the same limit, k may be identified as the stress concentration factor for an isolated rigid inclusion in an infinite block of power-law matrix. Since α and σ_0 are merely scaling parameters, it is obvious that k can depend only on n and geometry, which may be represented by the inclusion shape. The same holds for q.

Returning to Eq. (2), let us suppose that A is known at any given V. If a fraction dv of the composite is now substituted by the rigid phase with the remote stress Σ held fixed, then by invoking the self-consistent assumption we may regard the new material to be an isolated rigid inclusion in an infinite block of homogeneous matrix obeying the power-law Eq. (2). Recall that, according to Eq. (4), the effect caused by a small amount of rigid second phase is a fractional reduction, equal to the product of q and the inclusion fraction, of the matrix strain rate. Then, by treating the composite before substitution as a power-law matrix this time, we write an analogy to Eq. (4) the fractional reduction of $\dot{E}$ after substitution as

$$d\dot{E}/\dot{E} = -q\,dv \tag{6}$$

In the above we have utilized the previously stated result that q is independent of α and σ_0. To proceed further, we note that a fraction of the material replaced was already rigid. Therefore, the actual increment of inclusion fraction dV and the substitution dv are related by the following relation:

$$(1 - V)\,dv = dV \tag{7}$$

Thus

$$d\dot{E}/\dot{E} = -q\,dV/(1 - V) \tag{8}$$

which gives, after integration

$$\dot{E} = (1 - V)^q\alpha(\Sigma/\sigma_0)^n \tag{9}$$

This is just the form that we mentioned before (Section II(1)) with $A = (1 - V)^q$.

Since q is independent of V, the determination of q as a function of n and the shape of inclusion will complete the analysis.

(3) Stress Concentration Factors

(A) Equiaxed Inclusions: Using the variational principle, Duva[16] treated the spherical rigid inclusion problem. We have fitted his numerical result for q with the following equation:

$$q = 2 + n/2 \tag{10}$$

for n between 1 and 10, with good accuracy. This gives a stress concentration factor

$$k = 3/2 + 1/n \tag{11}$$

When $n = 1$, $k = 5/2$ in agreement with the Eshelby solution (Poisson ratio = 1/2 for incompressible material).[10] At large n, k decreases because of the progressively less strain (or strain rate) hardening in a power-law material. In the nonhardening limit (n being infinity), $k = 3/2$, which coincides with the finite difference and finite element solutions of a circular rigid inclusion in two dimensions.[17,18]

We will use in this paper the above result for both spherical and equiaxed inclusions. The composite follows a power law according to Eq. (5)

$$\dot{E} = (1 - V)^{2+n/2}\alpha(\Sigma/\sigma_0)^n \qquad \text{(equiaxed)} \tag{12}$$

The same equation was given by one of us previously without derivation.[5]

(B) Perpendicular Fibers: If a fiber is perpendicular to the tensile stress direction, its stress concentration should be relatively similar to that of a spherical inclusion. (Recall when $n = 1$, $k = 2.5$ for a sphere and $k = 2$ for a circular cylinder when loaded in tension along the short symmetry axis,[10,15] when n is infinite, $k = 1.5$ in both cases as noted before in Section II(3)(A).) Following this argument, we will assume that Eq. (12) applies.

(C) Parallel Fibers: Consider a rigid fiber of a radius R and a half length L in a power-law matrix. The fiber is paral-

lel to the stress direction. In the nonhardening (perfect plastic) limit, the deformation field contains a localized shear zone at the fiber/matrix interface but is otherwise uniform away from there. Within the shear zone, the shear stress τ is just one-half of the tensile flow stress, which is σ_0 in the absence of hardening. Such shear traction transfers a load from the matrix to the fiber, as described by the standard shear-lag analysis[19]

$$d\sigma_f/dz = -2\tau/R \tag{13}$$

Here σ_f is the fiber tensile stress at a distance z from the center. After integration, we obtain

$$\sigma_f(z) = \sigma_f(L) + 2\tau(L - z)/R \tag{14}$$

where $\sigma_f(L)$, the fiber stress at the end, can be identified with the flow stress of the matrix in uniaxial tension, i.e., σ_0. Meanwhile, the average stress within the fiber is

$$\langle\sigma_f\rangle = \sigma_f(L) + \tau L/R \tag{15}$$

Therefore, the stress concentration factor is

$$k = \langle\sigma_f\rangle/\sigma_0 = 1 + L/2R \qquad (1/n = 0) \tag{16}$$

In the above derivation, we have assumed that fibers are sufficiently strong to sustain the stress concentration without fracture.

By inspecting Eqs. (11) and (16), it becomes evident that the simplest expression of stress concentration factor which gives the correct results in two limiting cases, $1/n = 0$ for all L/R and $L/R = 1$ for all n, is

$$k = 1 + (1/2 + 1/n)(L/R) \tag{17}$$

Although the above result is only an approximate interpolation, we shall assume in this paper that it is adequate.

Using Eq. (5), q can be obtained readily. The composite containing parallel fibers along the tensile stress direction then follows a power law

$$\dot{E} = (1 - V)^{1+(1+n/2)(L/R)}\alpha(\Sigma/\sigma_0)^n \qquad \text{(parallel fibers)} \tag{18}$$

Because of the anisotropy caused by the fiber texture, additional constitutive relations, not developed here, are required to fully describe deformation under other loading conditions.

(D) Random Fibers: Consider the case of a composite in which fibers are randomly oriented. The simplified picture adopted here assumes that, on average, along any direction, approximately one-third of the fibers may be regarded as aligned along it, while the other two-thirds perpendicular to it. Using this picture, the average stress concentration factor for an assemble of random fibers in uniaxial tension may be taken as one-third of Eq. (17) plus two-thirds of Eq. (11), i.e.

$$k = 3/2 + 1/n + 1/3(1/2 + 1/n)(L/R - 1) \tag{19}$$

The composite containing random fibers follows a power law

$$\dot{E} = (1 - V)^{1+(1+n/2)(2/3+L/3R)}\alpha(\Sigma/\sigma_0)^n \qquad \text{(random fibers)} \tag{20}$$

(4) Numerical Results

The stress concentration factors as a function of stress exponent and aspect ratio of inclusions are plotted in Fig. 1, and the strain rates of the composite as a function of volume fraction of inclusions are plotted in Fig. 2. It is apparent from these results that stress concentrations are most severe in Newtonian flow, in parallel fibers of a high aspect ratio. On the other hand, flow reduction by a rigid phase in a non-Newtonian creeping material is more drastic than in a Newtonian material. Strengthening by equiaxed inclusions becomes significant only at higher volume fractions.

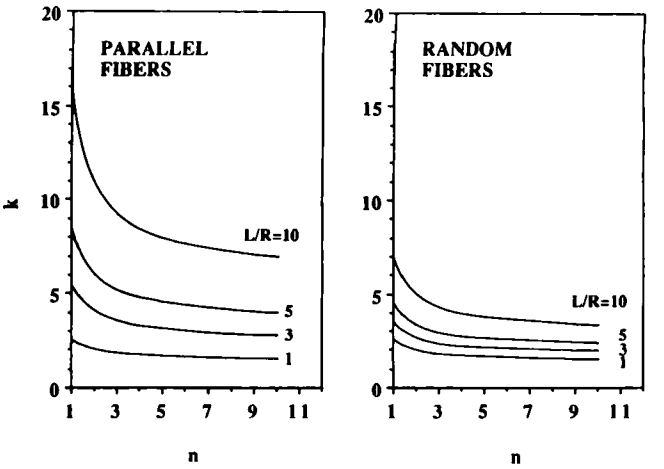

Fig. 1. Stress concentration factor k as a function of stress exponent n with two different orientation distributions of rigid fibers. The lowest branch, with $L/R = 1$, also corresponds to equiaxed inclusions.

III. Experimental Procedure

(1) Materials

The zirconia used in our study was a 2Y-TZP. For mullite, three compositions were investigated. The first two had molar Al_2O_3/SiO_2 ratios of 1.77 and 1.97, corresponding to 75 and 77 wt% Al_2O_3, thus designated as 75A and 77A, respectively. Mullite grains of this composition were equiaxed at all volume fractions. The third one had a molar Al_2O_3/SiO_2 ratio of 1.25, corresponding to 68 wt% Al_2O_3, thus designated as 68A. Mullite of this composition develops an elongated, short-fiber-like morphology.

Mullite powders were prepared using a solution of aluminum nitrate† and tetraethoxysilane† with ethanol, from which precipitates were formed by adding ammonia. The coprecipitated powders were calcined at 1000°C, then attrition-milled. A commercial 2Y-TZP‡ was added to the mullite powders, and the mixture was attrition-milled in water with a surfactant. In the above procedure, the alumina and silica pickup from milling media was monitored and compensated for accordingly by adjusting the starting composition. The milled slurry was cast under a pressure of 0.7 MPa into cakes which were dried and isostatically pressed at 175 MPa. Nearly theoretical densities (less than 2% porosity) were obtained after sintering in air at 1400°C for 1 h.

Annealing at the same temperature in air for up to 20 h was also performed to coarsen the grain size. In addition, to coarsen the mullite size more, we introduced different firing times when preparing special composites for the study of inclusion size effect. Using these methods, zirconia/mullite composites of various microstructures were obtained. The work reported here covers mullite volume fractions between 0 and 0.5 and aspect ratios between 1 and 5.

(2) Procedures

Square bar specimens of dimensions 2 mm × 2 mm × 4.6 mm were prepared for deformation experiments. Deformation was conducted in uniaxial compression to minimize the effect of cavitation on constitutive behavior. All tests were conducted in air, between 1250° and 1380°C, in a platinum furnace. SiC platens were used and found satisfactory with little evidence of end friction detectable even at very high strain rates. Most tests were run using a constant displacement rate. The axial displacement was recorded with an extensometer outside the furnace. By comparing its reading

†Alfa Products, Danvers, MA.
‡Tosoh Co., Tokyo, Japan.

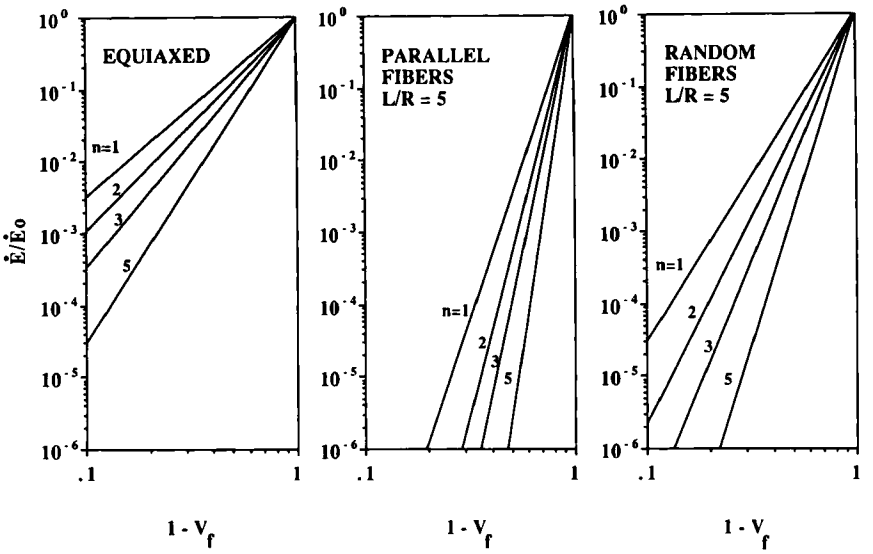

Fig. 2. Strain rate reduction factor, $\dot{E}/\dot{E}_0$, as a function of volume fraction of inclusions (fibers), V_f.

with the dimensions of the specimen after the test, the error was found to be within 2%. The load and displacement readings were converted into true stress and true strain rate data reported below. Since steady-state deformation could be reached with strains of the order of a few percent, a single specimen was often used for flow stress determinations at two to three increasing displacement rates. Typically, a test lasted no more than 1/2 h at the test temperature, terminated after reaching a height reduction of up to 50%. Under these circumstances, very little grain growth, if any, was found in deformed specimens.

X-ray diffraction was used both for phase identification and for verification of composition by precision determination of lattice parameters. Microstructures and textures were examined by scanning electron microscopy and X-ray diffraction. Grain size was taken as 1.56 times the linear intercept length of zirconia grains. Mullite grain size was also measured. The average aspect ratio from 100 of the most elongated mullite grains in a region of a polished section was determined. The value thus obtained would be fairly accurate if all mullite grains have the same aspect ratio in three dimensions. However, if a bimodal distribution of aspect ratio exists, then the above method could yield a substantial overestimation. The consequence of this complication will be discussed later, along with experimental results.

IV. Experimental Results and Analysis

(1) Microstructures

Microstructures of four sintered zirconia/mullite composites, containing 0 to 50 vol% mullite, are displayed in Fig. 3, in which mullite is shown as the darker grains. No intragranular phases, either zirconia or mullite, were found in these ceramics. The grain size of the as-sintered material became finer as volume fractions of two phases approached each other. Annealing at the sintering temperature for various times resulted in coarser grains of sizes up to 0.8 μm. No abnormal grain growth was found after such treatment. Only tetragonal zirconia and mullite, but not cubic zirconia or zircon, were found by X-ray diffraction after sintering, annealing, or compression.

Grain sizes of both mullite and zirconia remained constant after deformation. Indeed, a slight grain refinement was sometimes detected, presumably due to the breakup of the initial clusters of fine grains during deformation. No cavitation was evident even for heavily deformed specimens such as the ones shown in Fig. 4. Thus, microstructures of our specimens may be regarded as nearly constant during superplastic deformation.

Microstructural data and designations of the majority of sintered and annealed materials are summarized in Table I. Some relevant information on microstructures will be provided when deformation data are discussed. Further details of the deformed microstructures pertaining to textures, defects, and microanalysis will be reported elsewhere.

(2) 2Y-TZP and Mullite

Deformation data of the matrix, 2Y-TZP, are shown in Figs. 5 to 7. A stress exponent of $n = 1.54$, corresponding to a strain rate sensitivity $m = 1/n = 0.65$, was determined from Fig. 5 at all temperatures. Wakai and co-workers[20] have recently studied this material with a grain size of 0.3 μm. His data, shown in Fig. 6 as open circles, compare well with ours in both the temperature dependence and the order of magnitude, as evident from Fig. 6. The grain size dependence at 1380°C is shown in Fig. 7, also giving a similar stress exponent ($n = 1.56$ or $m = 0.64$). Considering the relatively low stress exponent even at very high strain rates, up to 4×10^{-3}/s in some tests, 2Y-TZP is a superplastic ceramic indeed.

We have also tested mullite of a grain size of 0.3 μm, sintered at 1550°C. No appreciable deformation was found at stresses up to 500 MPa, when it fractured at 1380°C. Previous studies by Dokko *et al.*[7] and Nixon *et al.*[21] reported that, in the diffusional creep regime, mullite's strain rate was inversely proportional to (grain size).[2] By extrapolating Dokko *et al.*'s data to smaller grain sizes, as in the case here, we found that the strain rate of mullite would be at least 3 orders of magnitude slower than that of 2Y-TZP in all the composites studied here.

(3) Effect of Volume Fraction

When mullite (75A) was added to 2Y-TZP, a similar stress exponent was obtained. The dependence of strain rate on the grain size (d) of zirconia, characterized by $p = \delta \ln \dot{\varepsilon}/(\delta \ln d)$, increased from ~2 in 2Y-TZP to ~3 in the composites, as shown in Fig. 8. The change in p is apparently due to a change in the material characteristics. Such effect is beyond the realm of the continuum theory given in Section II. Nevertheless, we can proceed with an approximate analysis of the constitutive relation by focusing first on the data of mullite containing composites. Thus, to account for the grain size dependence of strain rate, we multiply strain rates by $(d/0.2\ \mu\text{m})^3$ and plot them against stress for all composites in

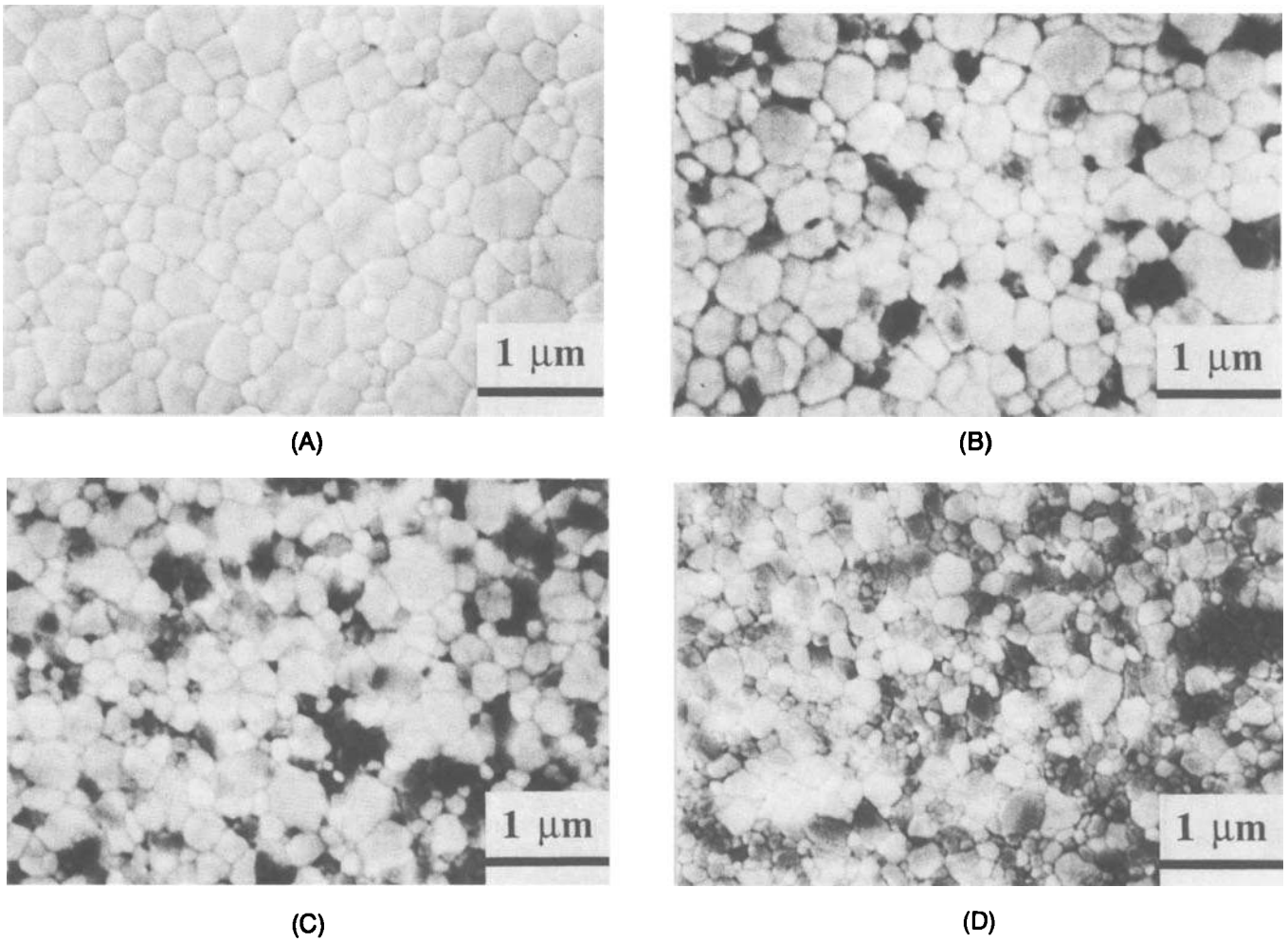

Fig. 3. Microstructures of as-sintered zirconia/mullite composites containing (A) no mullite, (B) 10 vol% mullite, (C) 30 vol% mullite, and (D) 50 vol% mullite.

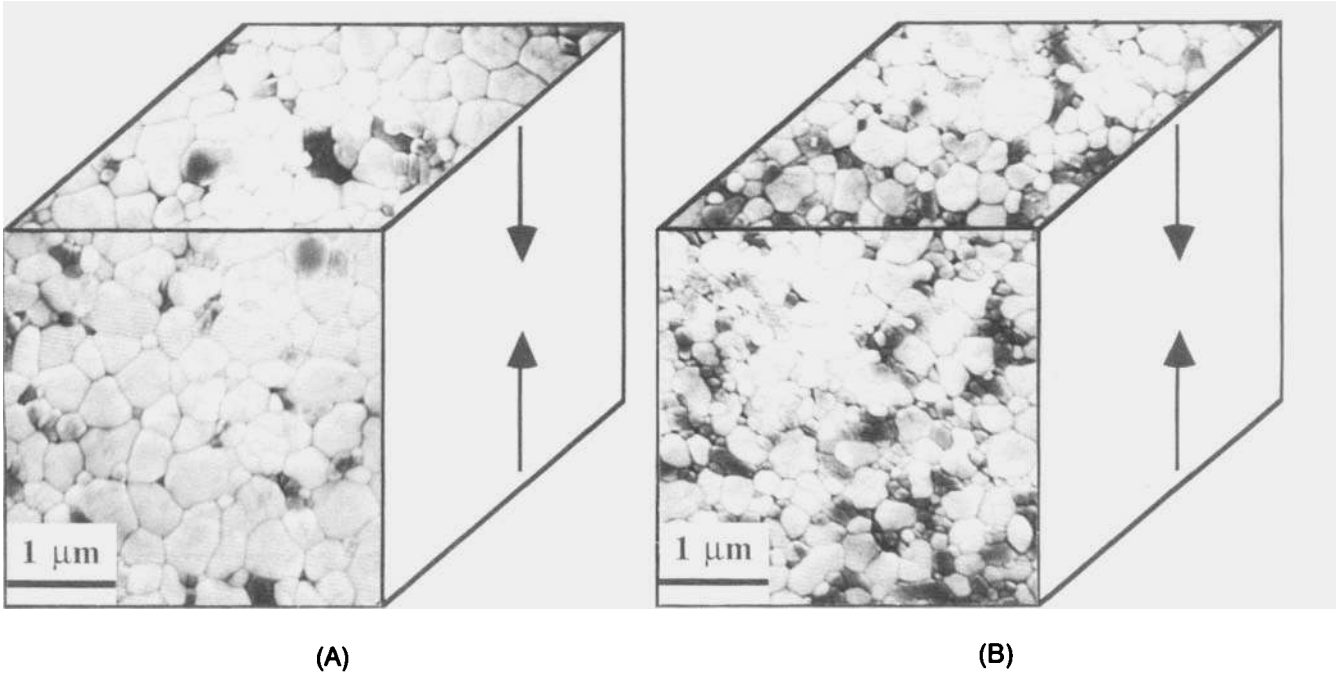

Fig. 4. Microstructures of deformed zirconia/mullite composites at 1350°C in two cross sections. (A) 10M–90Z; (B) 50M–50Z. The compression direction is indicated. $\varepsilon = -0.7$, $\dot{\varepsilon} = 6 \times 10^{-3}$/s

Table I. Firing Conditions and Grain Sizes of Composites

Composites†	Firing conditions		Grain size (μm)‡	
	Sintering	Annealing	Mullite	ZrO_2
0M–100Z	1400°C/1 h			0.39
		1400°C/9 h		0.54
		1400°C/39 h		0.67
10M–90Z	1400°C/1 h		0.18	0.43
		1400°C/9 h	0.23	0.55
		1400°C/19 h	0.48	0.83
	1400°C/1 h§		0.46	0.46
30M–70Z	1400°C/1 h		0.19	0.31
		1400°C/9 h	0.25	0.43
		1400°C/19 h	0.40	0.60
	1400°C/1 h§		0.56	0.36
50M–50Z	1400°C/1 h		0.21	0.23
		1400°C/9 h	0.31	0.33
		1400°C/19 h	0.42	0.46

†For example, 50M–50Z is a mixture of 50 vol% mullite with 75 wt% alumina and 50 vol% 2Y-TZP. ‡For mullite inclusion size effect study. §Grain size = linear intercept length × 1.56.

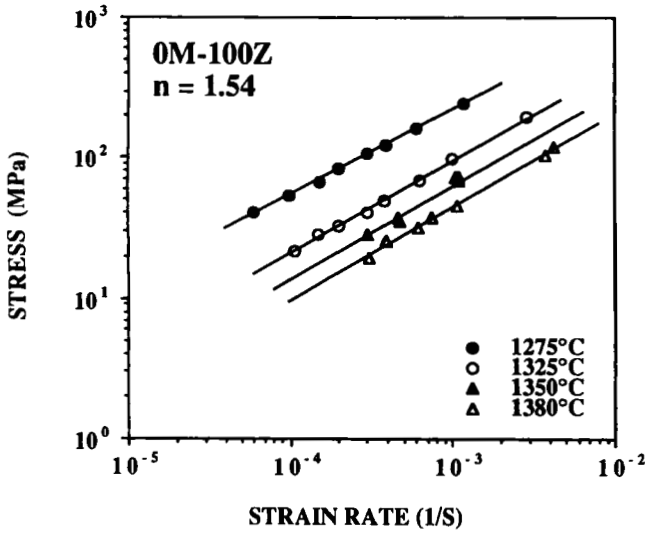

Fig. 5. Stress versus strain rate of 2Y-TZP at various temperatures. Grain size = 0.39 μm.

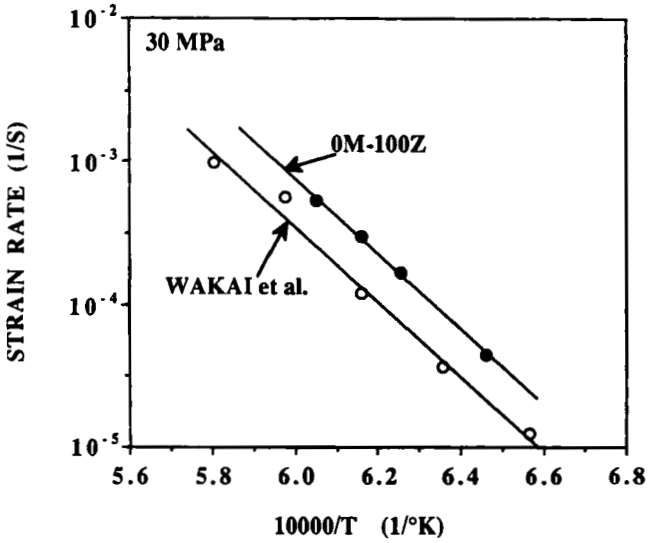

Fig. 6. Strain rate versus reciprocal temperature of 2Y-TZP deformed at 30 MPa.

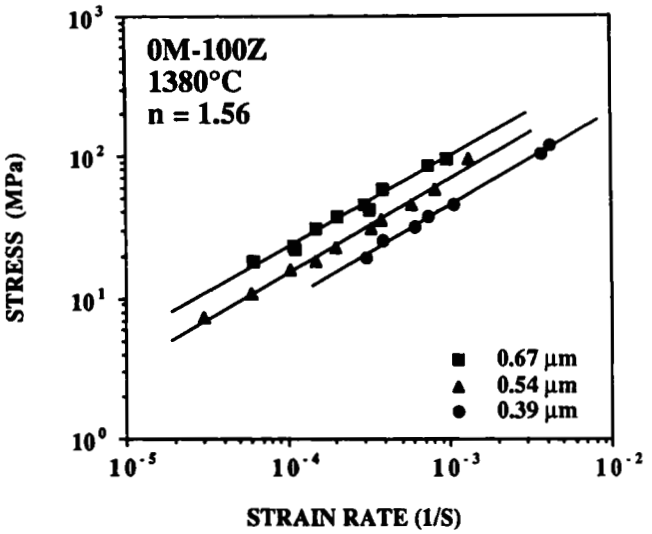

Fig. 7. Stress versus strain rate of 2Y-TZP at various grain sizes.

Fig. 9. The strain rate sensitivities obtained from these data range from 0.68 to 0.74 at 1350°C.

Data at other temperatures were similarly analyzed. From such analysis the activation energy Q was determined. Its value, as shown in Fig. 10, is affected by the mullite content. Once again, this is due to a change in the material characteristics and not predicted by the continuum theory, although the trend of Q is qualitatively understandable since diffusional creep of mullite has a much higher activation energy.[7] To proceed with the analysis of the constitutive relation, we can multiply strain rates by $(d/0.2\ \mu m)^3$ as before and by $\exp[(Q/R)(1/T - 1/1573\ K)]$ to account for their temperature dependence where R is the gas constant. In this way, data of different grain sizes and temperatures but of identical composition fall onto a straight line as shown in Fig. 11. It seems clear that a common stress exponent, $n = 1.50$ or $m = 0.67$, can describe all the data quite well.

Figure 11 also demonstrates the strengthening effect of mullite additions on the composites throughout the range of deformation conditions studied in this work. At a constant stress, temperature, and grain size, e.g., 70 MPa, 1350°C, and 0.2 μm, the suppression of superplastic flow by mullite is made apparent by plotting strain rate versus volume fraction of mullite. Such a plot is given in Fig. 12, in which the prediction of our model, Eq. (12) with $n = 1.5$, is shown as the

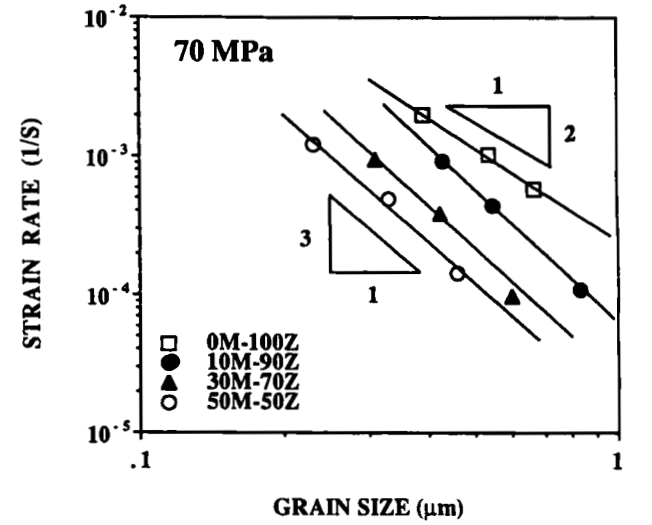

Fig. 8. Zirconia grain size dependence of strain rate for zirconia/mullite composites.

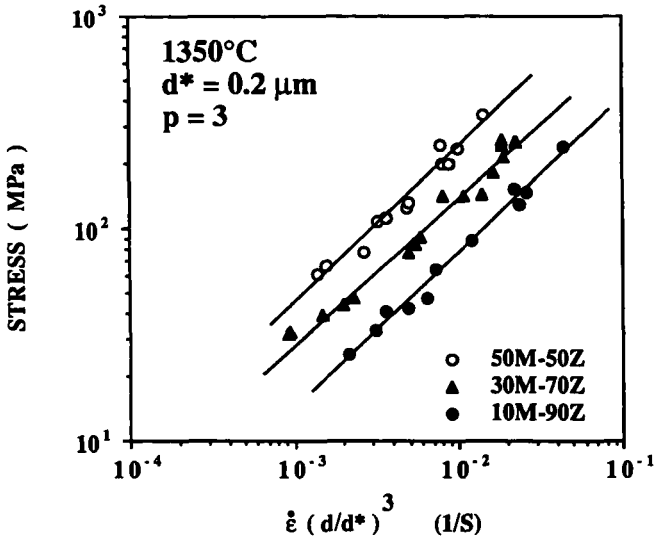

Fig. 9. Stress versus strain rate normalized by the grain size for zirconia/mullite composites.

straight line. The agreement is fairly good, considering the range of volume fractions covered, in particular at $V = 0.5$ when mullite grains are interconnected to some extent.

The above analysis suggests the following form of constitutive equation for superplastic zirconia (2Y-TZP)/mullite (75A) composites, as a function of temperature, grain size, and volume fraction

$$\dot{E} = [(1 - V_{\text{mullite}})^{2+n/2} C \Sigma^n \exp(-Q/RT)]/d^p \qquad (21)$$

where $n = 1.5$, $p = 3$, $Q = 700$ kJ/mol, and $C = 4.2 \times 10^{-3}$ m^3/(s·MPa$^{1.5}$) from the above analysis. When normalized using this equation to a reference temperature $T^* = 1300$°C and a reference grain size $d^* = 0.2$ μm, all the data of 2Y-TZP and its composites fall onto a single straight line with a correlation factor of 0.95, as shown in Fig. 13. To check the self-consistency of this representation, we note that the slope of Fig. 13 is 0.65, corresponding to $n = 1/m = 1.54$. Thus, notwithstanding some variations in the stress exponent, grain size dependence, and activation energy with mullite addition, a simple constitutive law consistent with our theory as given by Eq. (12) has been verified.

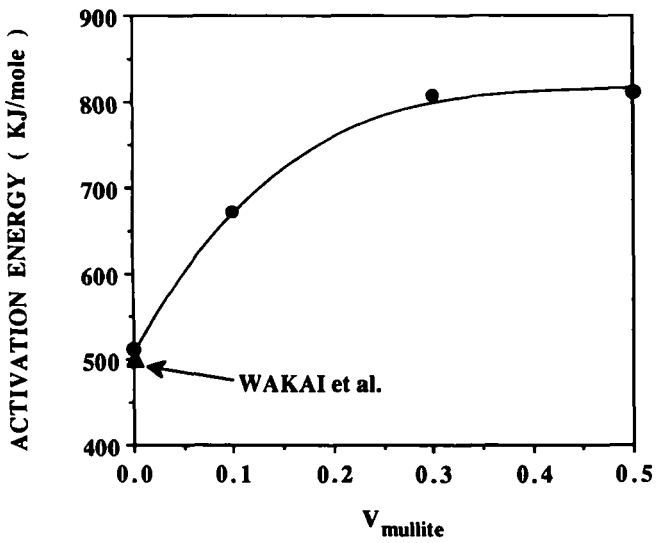

Fig. 10. Activation energy of superplastic flow versus volume fraction of mullite.

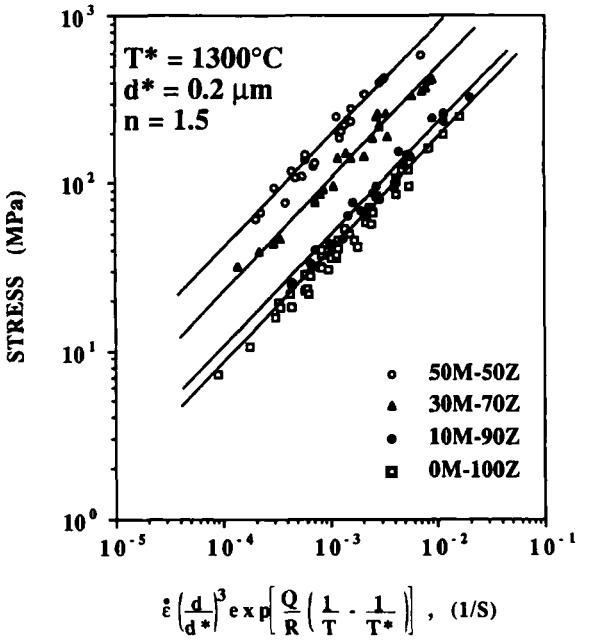

Fig. 11. Stress versus strain rate normalized by the grain size and temperature for four zirconia/mullite compositions.

(4) Effect of Aspect Ratio

A zirconia/mullite (68A) composite containing equal volume fractions of both phases was studied. After sintering for 1 h at 1400°C, the composite has a microstructure very similar to that of Fig. 3(D)(75A) except for a slightly larger grain size. However, after annealing at 1400°C for 20 h, many mullite grains in this silica-rich composite grew into elongated needles. A comparison of the microstructures of 77A and 68A composites after annealing for 20 h is seen in Fig. 14. The average aspect ratio of mullite grains, measured using the procedure described in Section III(2), was 5 in 68A composite. After the same annealing, mullite grains in 77A composite were larger but still equiaxed. No texture of mullite grains was observed after sintering either by electron microscopy or by X-ray diffraction.

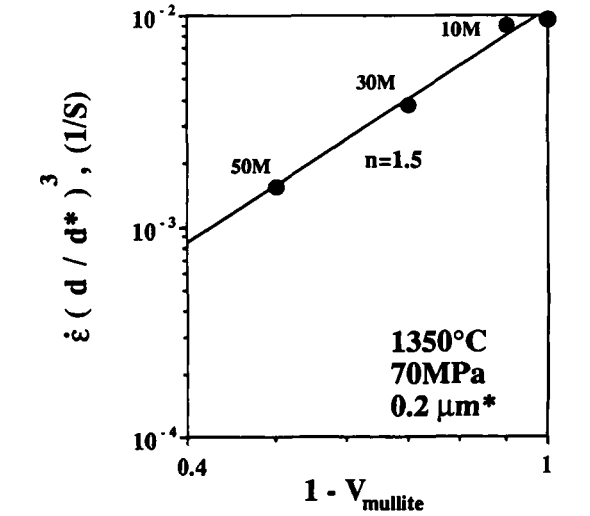

Fig. 12. Strain rate, normalized by the grain size, versus the volume fraction of mullite. The straight line is the model prediction of Eq. (12) with $n = 1.5$, assuming mullite inclusions are the rigid phase of an equiaxed shape.

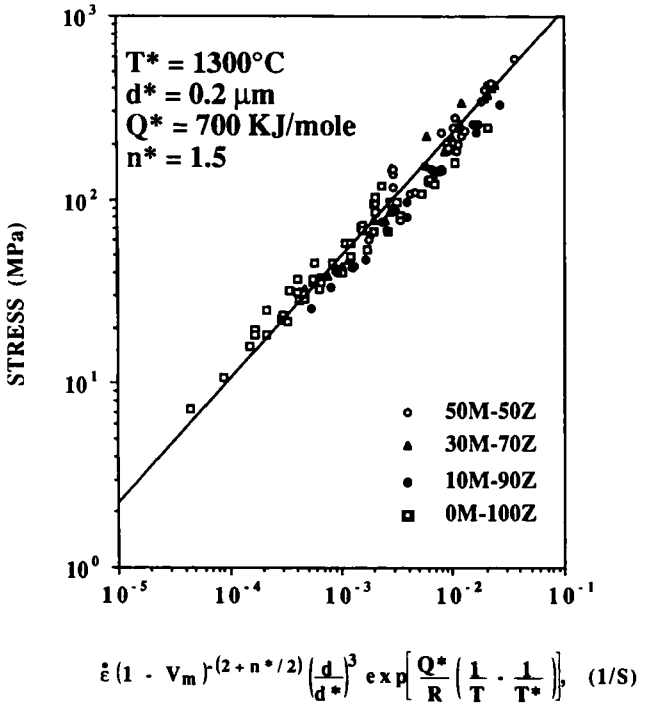

Fig. 13. Stress versus strain rate, normalized by the grain size, temperature, and the volume fraction of mullite (V_m) using Eq. (21), for four zirconia/mullite compositions.

We compared the deformation behavior of 68A composite and 77A composite in both the as-sintered state and the annealed state (Fig. 15). The slight difference of grain size of zirconia in these two materials has been taken into account in plotting data. Very similar stress exponents were obtained for all four materials. Comparing data when mullite grains were still equiaxed (1-h sintering), we found the 68A composite to deform faster, by a factor of 2, presumably due to its higher silica content which may have favored the formation of a grain-boundary glassy phase. However, this compositional advantage of 68A composite was lost after elongated mullite grains were developed, as indicated by the overlapping data of 68A and 75A composites (20-h annealing). We interpret the latter result as evidence for a more effective load transfer to the rigid phase of a higher aspect ratio. Coincidentally, in the special case considered here, these opposing compositional and shape effects just compensated each other fully in 68A and 75A composites after 20-h annealing.

Assuming the same compositional advantage, responsible for a flow enhancement by a factor of 2, as in the case of 1-h sintering, we may infer that the opposing flow suppression due to the shape change from $L/R = 1$ to $L/R = 5$ to be a factor of 2 as well. According to Eqs. (12) and (20), the flow suppression factor with equiaxed particles is $(1 - V_{mullite})^{2.75}$ at $n = 1.5$. With elongated but random particles, the flow suppression factor should be $(1 - V_{mullite})^{5.08}$ for $L/R = 5$. Since $V_{mullite} = 0.5$ in the present case, the predicted additional flow suppression accompanying the shape change, which can be estimated by taking the ratio of the above two predictions, is a factor of 5. This value is higher than the one inferred from our experiment. Indeed, our calculation found an increase of L/R from 1 to 2 to be sufficient to account for the experimental observation.

Two reasons are probably responsible for the discrepancy on the strengthening effect of short fibers in the present experiment. First, Fig. 14 indicates that mullite grains need to grow somewhat before becoming elongated, yet even after 20-h annealing at 1400°C some grains might still be too small and thus remained equiaxed. With a bimodal distribution of grain shapes, the procedure we used to establish the aspect ratio could have yielded an overestimate. Consequently, the flow suppression was overestimated too. This interpretation finds some support in Fig. 14 in which many small equiaxed mullite grains are visible in the annealed 68A composite. The second reason could be reorientation of mullite grains away from the stress axis during compression. Direct evidence of particle reorientation is offered in Fig. 16(A), which shows mullite grains preferentially lying perpendicular to the stress axis after large deformation. This phenomenon was further verified by a texture analysis from X-ray diffraction data, also shown in Fig. 16(B). Since the initial orientation of mullite grains was random, such reorientation caused a "geometrical softening"[§] effect, for perpendicular fibers are not as effective as aligned fibers in carrying the load. Indeed, if all the fibers were perpendicular to the compression axis, the flow suppression would be the same as that of equiaxed particles (Section II(3)(B)). (We may likewise expect tensile deformation to cause an opposite effect of "geometrical hardening,"[§]

[§]The term "geometric hardening/softening" is commonly used to describe the effect associated with rotations of crystallographic planes during slip.[22] In view of the analogy between resolved shear stress on the slip plane and the shear traction on the fiber/matrix interface, we have chosen to use the same term here.

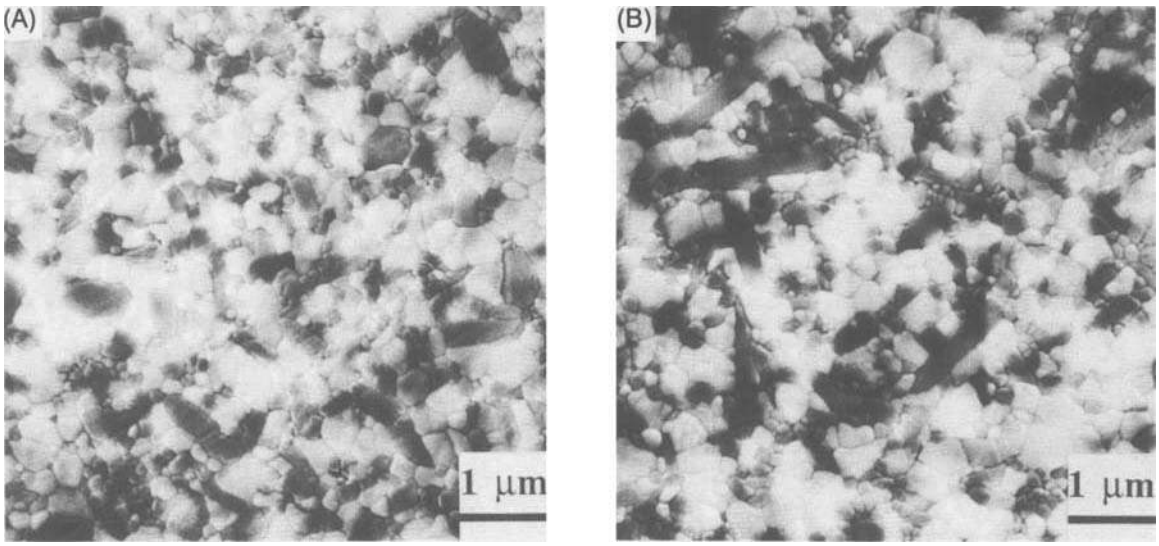

Fig. 14. Zirconia/mullite composites containing 50 vol% mullite after sintering at 1400°C for 20 h: (A) 50M–50Z (77A); (B) 50M–50Z (68A). The weight percent of Al_2O_3 is indicated in parentheses.

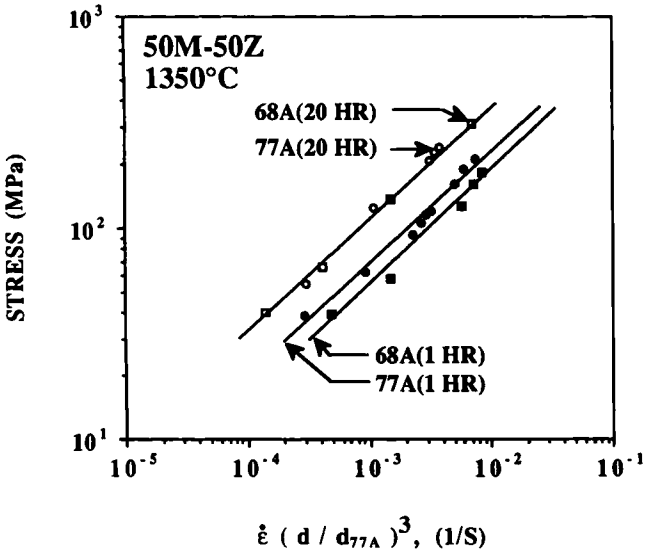

Fig. 15. Stress versus strain rate, normalized by the grain size for two zirconia/mullite composites of different mullite compositions and sintered for different times.

by fiber alignment along the tensile axis. In such case, flow suppression would increase as predicted by Eq. (18).

(5) Effect of Mullite Inclusion Size

As a final check on our theory, we investigated composites with mullite grains of different sizes. According to our continuum picture, composite flow should be insensitive to the size of the rigid inclusions. These experiments also provided a justification, a posteriori, of our use of zirconia grain size only in the representation of the constitutive relation (Section IV(3)).

Zirconia–mullite composites containing 10 and 30 vol% mullite were prepared by prefiring the mullite powders at 1600°C for 10 h before mixing. In samples containing 30 vol% mullite, a bimodal distribution of mullite inclusion size was observed. On a finer scale, mullite grains are comparable in size with the zirconia matrix grains, e.g., 0.4 μm (see Fig. 17(A)). On a coarser scale, an additional group of large equiaxed inclusions of a size of 150 μm were uniformly dispersed (see Fig. 17(B)). This composite, which contains coarse mullite grains, was found to deform with a slightly lower strain rate, by 20%, than a composite of the same composition but with only fine mullite grains, once the grain size effect of the zirconia was taken into effect. This comparison is illustrated by the upper two branches of data in Fig. 18. At a lower fraction of mullite concentration, i.e., 10 vol%, the mullite grains were mostly uniform in size and the deformations of composites containing mullite grains of different sizes were essentially indistinguishable from each other once the grain size effect of zirconia was taken into effect. These results are shown in Fig. 18 in the lower two branches of data. Considering the very large variation of mullite sizes studied, we conclude that the superplastic flow is not sensitive to the mullite grain size, in accordance with our continuum picture of rigid inclusions.

V. Discussion

Our theory predicts that flow reduction due to the presence of a rigid phase in a non-Newtonian creeping material is much more drastic than in a Newtonian material. This is apparent from an examination of Eqs. (12), (18), and (20) and Fig. 2 as a function of n. Interestingly, the model also predicts that stress concentration in a rigid inclusion is less in a non-Newtonian material than in a Newtonian material. This is apparent from Eqs. (11), (17), and (19) and Fig. 1. The reason that the stress concentration in rigid inclusions is less in a non-Newtonian matrix is directly related to the lesser hardening capability of such material. (In the limit of n being infinity, there is no hardening at all.) Thus, load transfer from matrix to inclusion is also less. On the other hand, since strain rate increases with stress in a power-law manner for non-Newtonian materials, the resultant flow reduction is more despite a less effective load sharing by rigid inclusions. These flow characteristics are unique to composites obeying a non-Newtonian constitutive relation.

The effect of rigid inclusions on superplastic deformation of a soft matrix was previously studied in an α/β brass by Suery and Baudelet.[23] As shown by Chen,[5] their data could be fitted to a form $E = (1 - V_\alpha)^{3.785}$, where V_α is the volume fraction of α phase which is rigid compared to β phase. Because of difficulties in obtaining a fine grain microstructure without a second phase, phase-pure β matrix was not tested to verify its superplastic characteristics. Wakai and co-workers[4] also investigated a soft/hard composite, e.g., 3Y-TZP with 20 wt% alumina, and found flow reduction. They used a previous version of our theory to interpret these results.[5] Unfortunately, in their analysis, which was done for only one volume frac-

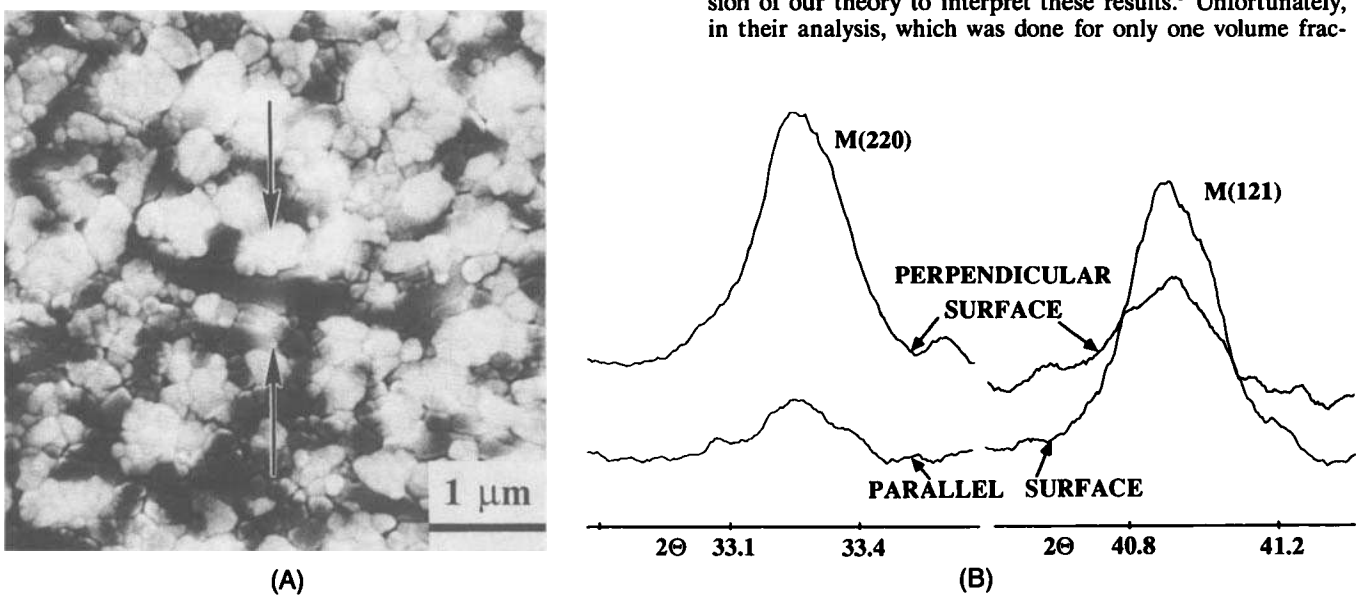

Fig. 16. (A) Deformed microstructures of 50M–50Z (68A) showing an elongated mullite grain lying normal to the compression axis, as indicated by arrows. (B) XRD patterns of the mullite reflections indicating a crystallographic texture.

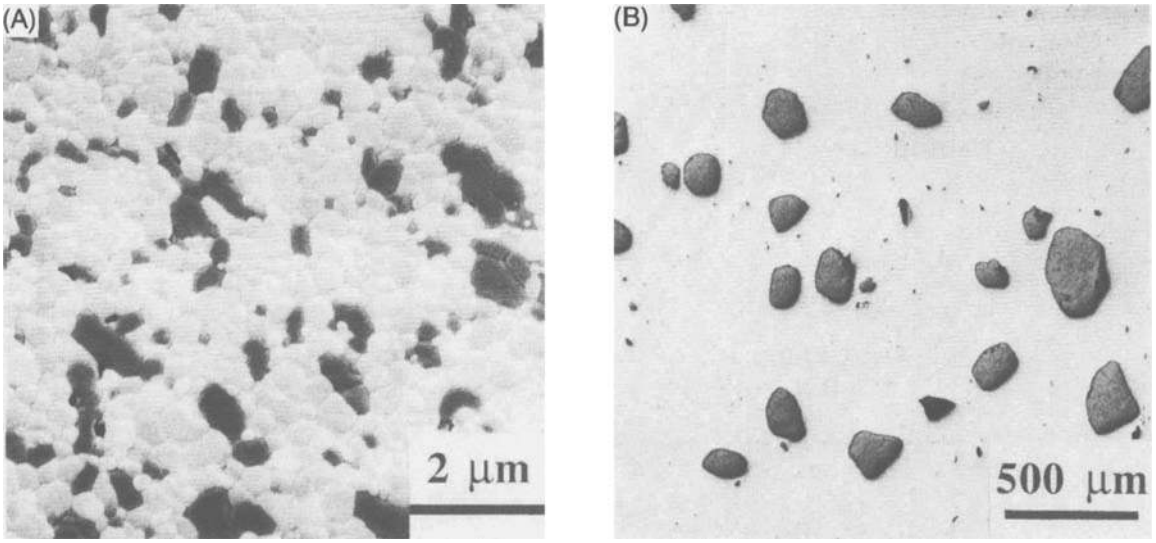

Fig. 17. Microstructures of a zirconia/mullite composite containing 30 vol% mullite: (A) small mullite inclusions, (B) large mullite inclusions.

tion, they had to assume alumina to be rigid, which was not strictly valid under their deformation conditions. Covering a wider range of composition in a more ideal model system, the present work on zirconia/mullite composites has provided a rigorous test of the composite theory presented in Section II. At least for equiaxed inclusions, the agreement seems to be good. For nonequiaxed inclusions, the agreement is qualitative at the present time, for reasons related to stereographical and geometrical complications as discussed in Section IV(4).

Application of the present description of two-phase flow is not limited to superplasticity. It can be adopted for non-Newtonian fluid flow with solid particles or for creep flow of ceramic/ceramic composites. In applying this theory, readers are advised to first verify that the deformation mechanism remains unchanged by the addition of rigid inclusions, to be ascertained at least by the same stress exponent. It can also be applied to rate-independent phenomena, since the mechanics of stress–strain field and steady-state stress–strain rate field are formally the same in corresponding boundary value problems.

In retrospect, it is remarkable that composites with reinforcement particles as small as 0.2 μm, as in the present work, can be described by continuum plasticity theory, which

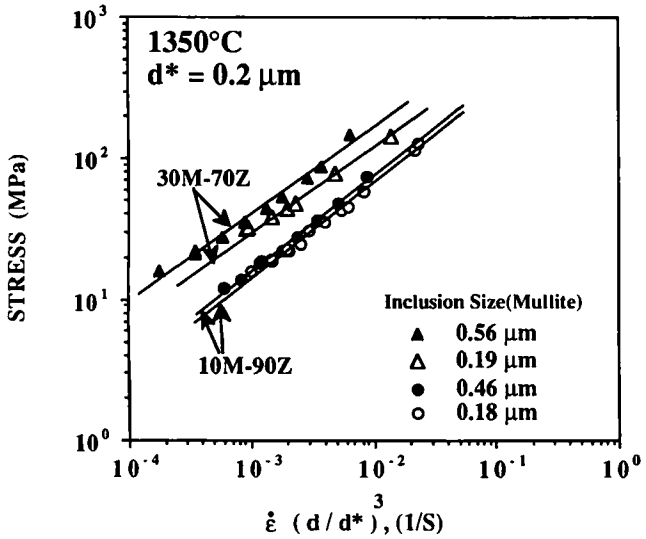

Fig. 18. Stress versus strain rate normalized by the grain size for two zirconia/mullite composites of different mullite inclusion sizes.

is often reserved for coarser microstructures in which the second phase is at least of a size of a few micrometers.[15,24] This size condition is thought to be necessary since finer inclusions may be small enough to interact with single dislocations for which the mechanics are nonlocal, as in the case of dispersion hardening. Only when the inclusions are so large that each interacts with "clouds" of dislocations is a continuum description appropriate. In the zirconia–mullite composite we studied, however, lattice dislocation mechanisms are not expected to operate. This can be verified by recalling two scaling "laws" which relate dislocation spacing λ and dislocation subgrain size D to flow stress[25]

$$\lambda/\mathbf{b} = 2G/\Sigma \tag{22}$$

$$D/\mathbf{b} = 100G/\Sigma \tag{23}$$

where $\mathbf{b}$ is the lattice Burgers vector (0.36 nm in zirconia) and G is the shear modulus (80 GPa in zirconia). (The numerical constants above are only approximate but regarded adequate for order-of-magnitude estimation.) Taking Σ to be 40 MPa, which is in the middle range of the stresses used in our study, we calculated λ and D to be 1.4 and 70 μm, respectively. These dimensions are much larger than the matrix grain size in our specimens, implying that superplasticity in the present material operates via a nondislocation, diffusional mechanism with a diffusion distance (grain size) much smaller than dislocation spacing.

Based on the above observation we may now state that the continuum picture is applicable under two circumstances: first, in dislocation creep when microstructures are much coarser than the dislocation cell size, and second, in diffusional creep and superplastic flow when microstructures are much finer than dislocation spacing. Of course, implicit in the continuum picture is that each constituent phase deforms according to its own constitutive relation, and that stress-driven kinetic demixing, due to different mobilities of common constituent atoms or ions shared by two phases, is not predominant. We have pointed out previously[5] that the application of the continuum picture may also be justified based on bounding theorems[26] specialized to diffusional creep problems, e.g., grain-switching problems[27] and inclusion problems.[28]

The zirconia/mullite composites reported in this study have not yet been tested in uniaxial tension. However, they have been stretched by a hemispherical punch in biaxial tension at 1350°C to large strains when the thin disk samples were supported on a ring. Since the latter deformation mode

is even more severe than uniaxial tension, we believe that it has adequately demonstrated the superplastic ductility of the material. Details of these experiments will be reported elsewhere.

VI. Summary

A. A continuum theory for non-Newtonian flow of a composite containing rigid inclusions in a power-law matrix has been developed. It predicts flow suppression by a factor of $(1 - V)^q$, q being a function of power-law exponent and inclusion shape. Stress concentrations in rigid inclusions have also been evaluated. As the stress exponent increases, flow suppression is more pronounced even though stress concentration is less.

B. Superplastic mullite/zirconia composites, containing submicron equiaxed grains of 2Y-TZP and alumina-rich mullite, deform according to the following constitutive equation

$$\dot{E} = [(1 - V_{\text{mullite}})^{2+n/2} C \Sigma^n \exp(-Q/RT)]/d^p \qquad (21)$$

where $n = 1.5$, $p = 3$, $Q = 700$ kJ/mol, and $C = 4.2 \times 10^{-3}$ $m^3/(s \cdot MPa^{1.5})$ in the temperature range of 1250° and 1380°C, with V_{mullite} up to 0.5. The dependence on the volume fraction of mullite can be quantitatively described by the continuum theory, in which the mullite phase is treated as nondeforming rigid inclusions. The mullite inclusion size was found to have little effect on deformation.

C. When the alumina-to-silica ratio in mullite was decreased to 1.25, the composite showed accelerated deformation if mullite grains were small and equiaxed. Prolonged annealing at 1400°C resulted in an elongated morphology for mullite, which strengthened the composite by a fiber-reinforcement mechanism. Deformation texture of these elongated inclusions was observed. The continuum theory was found to be in qualitative agreement with the strengthening data.

D. Superplastic flow in the present study had very little contribution from lattice dislocation mechanisms. This observation is based on scaling considerations of dislocation spacing and subgrain size, which are much larger than the very small grain sizes typically required for ceramic superplasticity.

Acknowledgments: We are grateful to Dr. Shuzu Kanzaki of the Government Industrial Research Institute, Nagoya, Japan for providing the elastic constant data of the mullite quoted in the Introduction and to his colleague, Dr. Fumihiro Wakai, for providing the creep data of 2Y-TZP quoted as Ref. 20.

References

[1]J.W. Edington, K.N. Melton, and C.P. Cutler, "Superplasticity," *Prog. Mater. Sci.*, **21** 61–170 (1976).

[2]F. Wakai, S. Sakaguchi, and Y. Matsuno, "Superplasticity of Yttria-Stabilized Tetragonal ZrO_2 Polycrystals," *Adv. Ceram. Mater.*, **1** [3] 259–61 (1986).

[3]F. Wakai, N. Murayama, S. Sakaguchi, H. Kato, and K. Kuroda, "Deformation of Superplastic Tetragonal ZrO_2 Polycrystals"; pp. 583–93 in Advances in Ceramics, Vol. 24, Science and Technology of Zirconia III. Edited by S. Somiya, N. Yamamoto, and N. Yanagida. American Ceramic Society, Westerville, OH, 1988.

[4]F. Wakai and H. Kato, "Superplasticity of TZP/Al_2O_3 Composites," *Adv. Ceram. Mater.*, **3** [1] 71–78 (1988).

[5]I-W. Chen, "Superplastic Flow of Two-Phase Alloys"; Ch. 5 in Superplasticity. Edited by B. Baudelet and M. Suery. Edition du CNRS, Grenoble, France, 1985.

[6]I-W. Chen, "Diffusional Creep of Two-Phase Materials," *Acta Metall.*, **30**, 1655–64 (1982).

[7]P.C. Dokko, J.A. Pask, and K.S. Mazdiyasni, "High-Temperature Mechanical Properties of Mullite Under Compression," *J. Am. Ceram. Soc.*, **60** [3–4] 150–55 (1977).

[8]R. Hill, The Mathematical Theory of Plasticity. Clarendon Press, Oxford, U.K., 1975.

[9]A. Einstein, "A New Determination of Molecular Dimensions" (in Ger.), *Ann. Phys. (Leipzig)*, **19**, 289 (1906).

[10]J. D. Eshelby, "The Determination of the Elastic Field of an Ellipsoidal Inclusion and Related Problems," *Proc. R. Soc. London, A*, **241A**, 376–96 (1957).

[11]R. Roscoe, "Isotropic Composites with Elastic or Viscoelastic Phases: General Bounds for the Moduli and Solutions for Special Geometries," *Rheol. Acta*, **12**, 404 (1973).

[12]S. Boucher, "Effective Modulus of Quasi-Homogeneous, Quasi-Isotropic Composite Materials Constituted of Elastic Matrix and Elastic Inclusions" II. "Case of Finite Concentrations of Inclusions" (in Fr.), *Rev. Metall. (Paris)*, **22**, 31–36 (1976).

[13]R. McLaughlin, "A Study of the Differential Scheme for Composite Materials," *Int. J. Eng. Sci.*, **15**, 237–44 (1977).

[14]M. P. Cleary, I-W. Chen, and S-M. Lee, "Self-Consistent Techniques for Heterogeneous Media," *J. Eng. Mech. Div., Am. Soc. Civ. Eng.*, **106** [EMS] 861–87 (1980).

[15]I-W. Chen and A.S. Argon, "Steady State Power-Law Creep in Heterogeneous Alloys with Coarse Microstructures," *Acta Metall.*, **27**, 785–91 (1979).

[16]J. M. Duva, "A Self-Consistent Analysis of the Stiffening Effect of Rigid Inclusions on a Power-Law Material," *J. Eng. Mater. Technol.*, **106** [4] October, 317–21 (1984).

[17]W. Huang, "Theoretical Study of Stress Concentrations at Circular Holes and Inclusions in Strain Hardening Materials," *"Int. J. Solids Struct.,"* **8**, 149 (1972).

[18]A.S. Argon, J. Im, and A. Needleman, "Distribution of Plastic Strain and Negative Pressure in Necked Steel and Copper Bars," *Metall. Trans. A*, **6A**, 815–24 (1975).

[19]H.L. Cox, "The Elasticity and Strength of Paper and Other Fibrous Materials," *Br. J. Appl. Phys.*, **3**, 72–79 (1952).

[20]F. Wakai; private communication, 1988.

[21]R.D. Nixon, S. Chevacharoenkul, R.F. Davis, and T.N. Tiegs, "Creep of Hot Pressed SiC Whisker Reinforced Mullite"; unpublished work.

[22]E. Schmid and W. Boas, Plasticity of Crystals, English Edition. F.A. Hughes and Co., London, U.K., 1950.

[23]M. Suery and B. Baudelet, "Hydrodynamical Behavior of a Two-Phase Superplastic Alloy: α/β Brass," *Philos. Mag. A*, **41** [1] 41–64 (1980).

[24]A.S. Argon, "Inelastic Deformation and Fracture of Crystalline Solids"; p. 383 in Surface Effects in Crystal Plasticity. Edited by R.M. Latanision and J.F. Fourie. Noordhoff International Publishing, Netherlands, 1977.

[25]S. Takeuchi and A.S. Argon, "Review—Steady-State Creep of Single-Phase Crystalline Matter at High Temperature," *J. Mater. Sci.*, **11**, 1542–66 (1976).

[26]R. Hill, "New Horizons in the Mechanics of Solids," *J. Mech. Phys. Solids*, **5**, 66–74 (1956).

[27]M.F. Ashby, G.H. Edward, J. Davenport, and R.A. Verrall, "Application of Bound Theorems for Creeping Solids and Their Application to Large Strain Diffusional Flow," *Acta. Metall.*, **26**, 1379 (1978).

[28]I-W. Chen; presented at Symposium on Superplastic Forming of Structural Alloys, San Diego, CA, June 21–24, 1982. □